

Resolving Contrasting Regional Rainfall Responses to El Niño over Tropical Africa

PRADIPTA PARHI

Department of Earth and Environmental Engineering, Columbia University, New York

ALESSANDRA GIANNINI

International Research Institute for Climate and Society, Earth Institute, Columbia University, New York

PIERRE GENTINE

*Department of Earth and Environmental Engineering, and Columbia Water Center,
Earth Institute, Columbia University, New York*

UPMANU LALL

Department of Earth and Environmental Engineering, International Research Institute for Climate and Society, and Columbia Water Center, Earth Institute, Columbia University, New York

(Manuscript received 22 January 2015, in final form 5 October 2015)

ABSTRACT

The evolution of El Niño can be separated into two phases—namely, growth and mature—depending on whether the regional sea surface temperature has adjusted to the tropospheric warming in the remote tropics (tropical regions away from the central and eastern tropical Pacific Ocean). The western Sahel's main rainy season (July–September) is shown to be affected by the growth phase of El Niño through (i) a lack of neighboring North Atlantic sea surface warming, (ii) an absence of an atmospheric column water vapor anomaly over the North Atlantic and western Sahel, and (iii) higher atmospheric vertical stability over the western Sahel, resulting in the suppression of mean seasonal rainfall as well as number of wet days. In contrast, the short rainy season (October–December) of tropical eastern Africa is impacted by the mature phase of El Niño through (i) neighboring Indian Ocean sea surface warming, (ii) positive column water vapor anomalies over the Indian Ocean and tropical eastern Africa, and (iii) higher atmospheric vertical instability over tropical eastern Africa, leading to an increase in the mean seasonal rainfall as well as in the number of wet days. While the modulation of the frequency of wet days and seasonal mean accumulation is statistically significant, daily rainfall intensity (for days with rainfall $> 1 \text{ mm day}^{-1}$), whether mean, median, or extreme, does not show a significant response in either region. Hence, the variability in seasonal mean rainfall that can be attributed to the El Niño–Southern Oscillation phenomenon in both regions is likely due to changes in the frequency of rainfall.

1. Introduction

In its warm phase (i.e., El Niño), El Niño–Southern Oscillation (ENSO) causes widespread warming and affects the atmospheric stability tropicwide on an

interannual time scale. Studies in the past have taken an idealized numerical modeling approach to explain the modulation of climate by El Niño–teleconnected tropospheric warming, but observational evidence has been limited for validating the mechanism, particularly for rainfall response over remote tropical land regions (Chiang and Lintner 2005; Chiang and Sobel 2002; Herceg et al. 2007), where “remote tropical land regions” refers to the tropical regions outside of the ENSO regions (central and eastern tropical Pacific Ocean). On the other hand, empirical studies (Davey et al. 2014; Ropelewski and Halpert 1987) identifying teleconnected regions abound but usually offer limited process-level

 Denotes Open Access content.

Corresponding author address: Pradipta Parhi, Department of Earth and Environment Engineering, Columbia University, 500 W. 120th Street, New York, NY 10027.
E-mail: pp2417@columbia.edu

DOI: 10.1175/JCLI-D-15-0071.1

understanding, without which confidence in future projections would be limited. In one study, [Tang and Neelin \(2004\)](#) showed how the growth response of El Niño–teleconnected tropospheric warming captured by a disequilibrium principal component of the North Atlantic sea surface temperature (SST) and tropospheric temperature leads to an increased stability of the atmospheric column, thus suppressing North Atlantic cyclogenesis. Very few such studies (e.g., [Tang and Neelin 2004](#)) have attempted to develop an explanation of the physical mechanisms related to El Niño–teleconnected tropospheric warming through observations.

Tropical Africa is a good target for such an empirical study from both scientific and societal perspectives with a hope to (i) advance our understanding of the uncertainties in climate projections and (ii) better manage climate risk for the vulnerable population. Detecting the ENSO signal in rainfall modulation over tropical Africa remains challenging, where multiple climate factors, such as the North Atlantic Oscillation (NAO), Atlantic multidecadal oscillation (AMO), Indian Ocean dipole (IOD), African easterly jet, tropical easterly jet, and Saharan heat low, confound and modulate rainfall at different time scales ([Nicholson 2013](#); [Okonkwo 2014](#)). Many prior studies have analyzed tropical African climate and enhanced our understanding of the mechanisms modulating rainfall response ([Camberlin et al. 2001](#); [Losada et al. 2012](#); [Mohino et al. 2011](#); [Paeth and Friederichs 2004](#); [Philippon et al. 2014](#); [Polo et al. 2008](#); [Rodríguez-Fonseca et al. 2011](#)). These studies have explained the physical mechanisms on a case-by-case basis, by characterizing the ENSO–teleconnected relationships with individual land regions such as the Sahel or tropical eastern Africa (TEA). However, there has been no study, to our knowledge, explaining the regional heterogeneity in remote tropical rainfall response based on a single, coherent physical mechanism. Furthermore, the above-cited studies have usually considered the mean rainfall response at monthly or seasonal time scales, while less attention has been given to the understanding of changes in other rainfall characteristics such as the frequency of wet days or the intensity of extremes, which are key for socioeconomic risk management (e.g., agriculture). Better understanding of El Niño teleconnection mechanisms and their heterogeneous remote tropical rainfall response as discussed in this paper is important both in the near and longer term.

In the near term (i.e., over the next few decades), the internal variability of the climate system may still explain most of the uncertainty in climate projections (note that uncertainty can arise from three main sources: emission scenario, climate model uncertainty, and

internal variability; [Hawkins and Sutton 2009](#)), and ENSO will remain a prominent feature of internal climate variability compared to global warming (GW). [Fischer et al. \(2013\)](#) found that internal variability may account for as much as 75% of the uncertainty of extreme rainfall projections to 2050 at local or regional scales.

In the longer term, GW might dominate in determining the fate of regional rainfall response. Hence, there is a need to understand how climate at the regional scale might evolve. In the current climate, warming due to El Niño and its teleconnected mechanisms can provide clues as to how regional climate would respond to GW ([Neelin et al. 2003](#)). Of course, El Niño–related warming is not a perfect analog for GW because of these important differences: (i) warming is initially localized near the surface in the ENSO region (tropical central and eastern Pacific Ocean), while it is planetary and not restricted to the surface in GW; and (ii) an important component of the atmospheric response to GW is related to changes in meridional thermal gradients, which are not the primary driver in ENSO. However, there are also some suggestions that El Niño events may be a partial analog for GW, particularly over the tropics. [Neelin et al. \(2003\)](#) proposed that the regional drought mechanisms that induce tropical rainfall changes in El Niño might similarly change tropical rainfall under GW, since El Niño creates large-scale tropospheric warming over the entire tropics similar to that expected from GW. Furthermore, [O'Gorman \(2012\)](#) showed that the extreme rainfall sensitivities of climate models over the tropics are similar in terms of both interannual variability and longer-term GW and suggested that insights from interannual variation such as ENSO could be used to constrain climate models to improve interpretation of GW projections. Several studies (e.g., [Meehl and Washington 1996](#); [Song and Zhang 2014](#); [Teng et al. 2006](#); [Yeh et al. 2012](#)) have also found an El Niño–like SST anomaly signature in GW simulations. Thus, insights gained from El Niño–related dynamics as suggested by the analyses presented in our paper may be relevant in interpreting the heterogeneous regional climate response of longer-term, slowly evolving GW.

We begin, in [section 2](#), by summarizing the teleconnection mechanism and our hypotheses. In [section 3](#), we summarize the datasets used. In [section 4](#), we briefly discuss the evolution of tropospheric temperature and sea surface temperature during the growth and mature phases of El Niño. We report on our daily rainfall analysis in [section 5](#). In [sections 6 and 7](#) we report on the analysis of column water vapor and vertical pressure velocity, respectively. Finally, in [section 8](#), we summarize and discuss our main findings and conclude.

2. ENSO teleconnection mechanism and hypotheses

We use gridded daily rainfall data derived from stations and satellites to show that a coherent teleconnection mechanism—a tropical tropospheric temperature (TT) mechanism, as suggested by [Chiang and Sobel \(2002\)](#), hereinafter [CS02](#)—explains the contrasting changes in rainfall characteristics at the regional scale in the remote tropics. [CS02](#) proposed that during El Niño a chain of events is triggered in the coupled tropical ocean and atmosphere. The anomalous warming of the central and eastern tropical Pacific Ocean drives an increase in deep moist convective activity and increases latent heat release in the free troposphere. Over the central and eastern tropical Pacific, this free tropospheric diabatic heating anomaly spreads both eastward by equatorial Kelvin waves and westward by Rossby waves to the remote tropical free troposphere at different lag times because the tropical atmosphere can only sustain weak temperature gradients ([Sobel et al. 2001](#)). Similar teleconnection ideas have been referred to as “atmospheric bridges” in the literature ([Alexander et al. 2002](#); [Klein et al. 1999](#)).

[CS02](#) characterized the evolution of the teleconnection in terms of three phases—growth, mature, and decay—based on the strength of lag–lead spatio-temporal correlations of TT with an ENSO index. We simplify the analysis and divide the evolution into two phases, depending on the lag time of the remote tropical SST adjustment response to TT warming, and refer to them as growth and mature phases, respectively. Our phase definition follows [CS02](#)'s since TT and SST are coupled particularly during the rainy season. Here, we hypothesize that the growth phase behavior is a “dis-equilibrium phase.” The growth phase generally occurs during the boreal spring and/or summer seasons after El Niño's onset and prior to El Niño's peak in boreal winter season. The precise months would vary regionally within the remote tropics, depending on (i) the onset time and strength of ENSO and (ii) how far the tropical region is from the ENSO region (i.e., central or eastern Pacific Ocean), where the tropical waves emanate. Typically Northern Hemisphere summer monsoons are affected during this phase ([Goswami and Xavier 2005](#); [Lyon and Barnston 2005](#); [Rajagopalan and Molnar 2014](#); [Xavier et al. 2007](#)). For example, the July–September (JAS) rainy season over the western Sahel coincides with this growth phase.

During the growth phase, moist convection is suppressed over the regional oceans in the remote tropics because of the increased stability imposed by warming at upper levels induced by tropospheric wave propagation of the TT anomaly. This upper-level warming is

communicated downward to the atmospheric boundary layer (ABL) through increased ABL warm air entrainment induced by the warmer free troposphere ([Gentine et al. 2013a,b](#)) since the free troposphere maintains a moist adiabatic lapse rate in active moist convective regions under the quasi-equilibrium regime ([Arakawa and Schubert 1974](#); [Emanuel et al. 1994](#); [Neelin et al. 2008](#)). In tandem, surface fluxes act to bring the ABL and ocean surface layer in equilibrium ([Emanuel et al. 1994](#)). However, because of the high thermal inertia of the ocean mixed layer and the local dissipation through ocean heat transport, the regional SST in the remote tropics does not warm up instantly during the growth phase of El Niño. This lack of regional SST warming in the remote tropics leads to an absence of any anomalous low-level moist static energy (MSE) over those regional oceans, as shown by [Johnson and Xie \(2010\)](#); the ABL MSE depends largely on SST, with the largest values over the highest SST since the relative humidity and air–sea temperature difference exhibit rather limited variability over tropical oceans. Yet, as the TT warming anomaly is communicated to the ABL and from the ABL to the ocean mixed layer, the regional SST in the remote tropics ultimately increases with a delay of a few months. We next discuss the implications for the remote tropical land regions by extending these mechanisms. Refer to a schematic (see [Fig. 1](#)) summarizing the mechanisms for both remote tropical ocean and land regions.

We hypothesize that similar responses as are described over remote tropical oceans may be observed in those remote tropical land regions where rainfall variability is controlled by both (i) the changes in low-level MSE or moisture supply due to changes in SST over the neighboring remote tropical ocean regions acting as the MSE or moisture source (note: SST and low-level MSE or moisture are coupled in tropical oceans) and (ii) the changes in SST over the ENSO region acting as the heating source of the tropical free troposphere. Thus, the main expected characteristics of an El Niño–teleconnected growth phase for the selected remote tropical land region are similar to those for the remote tropical oceans and can be summarized as (i) a lack of regional SST warming in the remote tropics, (ii) an absence of atmospheric column water vapor (CWV) anomaly over the remote tropical land region since there is no atmospheric CWV anomaly over the moisture source region in the neighboring remote tropical ocean, and (iii) higher atmospheric stability over the land induced from the top by TT warming, resulting in (iv) suppression of moist convection over the remote tropical land region.

The suppression of moist convection can manifest in terms of changes in number of wet days and/or other

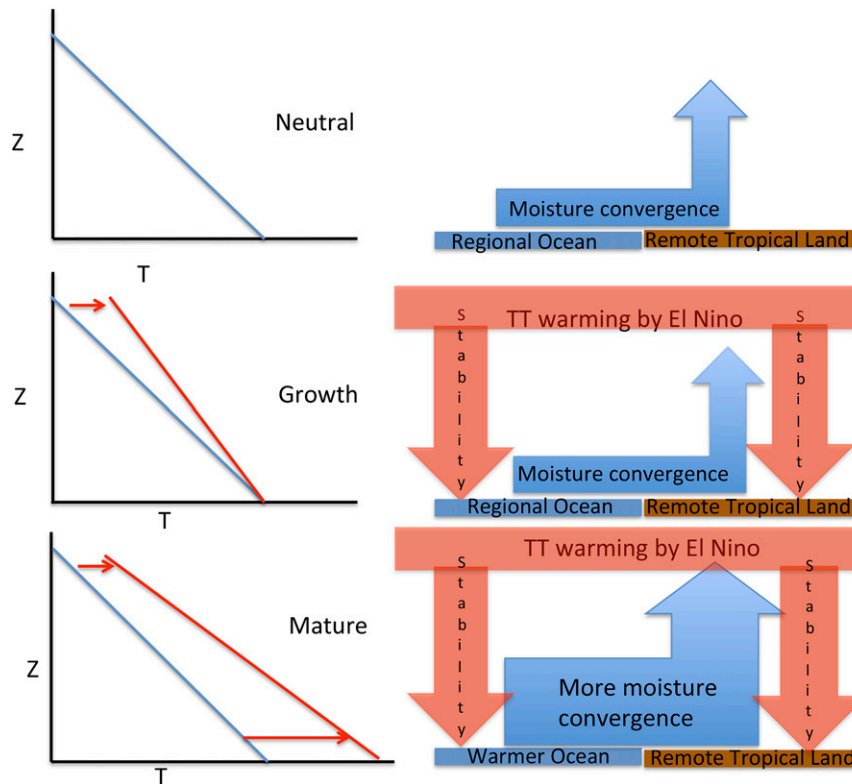


FIG. 1. Schematic showing our hypothesized TT mechanism acting upon remote tropical land and adjacent regional ocean (moisture source). (left) The environmental lapse rates are shown for the remote tropical land regions with temperature T on the x axis and height Z on the y axis. The lapse rate is shown in blue for the neutral case and in red for the El Niño case. Note how in the mature phase of El Niño the surface warming by moist static energy convergence increases the lapse rate (more negative slope). (right) The moisture and heat fluxes are shown for the remote tropical ocean and land region for (top) neutral, (middle) growth, and (bottom) mature cases. The thick red horizontal lines in the cases of growth and mature phase indicate the TT warming advection in the free troposphere. The blue arrows indicate the ocean-to-land moisture advection and convergence in the rainy season. For mature phase, the blue arrow is thicker suggesting the bottom-up instability dominates over the stability caused by the TT warming acting top down.

rainfall distribution characteristics such as mean, median, or extreme values. The frequency of days when the low-level moisture and associated MSE overcomes the upped ante should decrease. Briefly, the upped ante (Neelin et al. 2003) can be understood as the extra MSE required in the ABL to make the atmosphere convectively unstable when the tropical troposphere warms from either remote teleconnection effects during El Niño or increased infrared trapping by greenhouse gases in case of GW. This would suggest a decrease (increase) in the number of wet (dry) days in terms of frequency and a decrease in aggregated seasonal accumulation or mean. Despite higher atmospheric stability and moist convective suppression, the response of extremes is not clear since the rainfall intensity could also increase if the low-level moisture and MSE accumulated sufficiently

to a higher critical value. The MSE accumulation process would be favored if low-level MSE failed to dissipate upward as frequently as a result of upped ante or inhibition, assuming no significant changes in low-level entrainment or divergence. Since the MSE accumulation process is complex and difficult to establish a priori, we investigated different indices of rainfall representing both frequency and intensity.

Next, we hypothesize that the mature phase, which spans from the peak season [October–December (OND)] of El Niño to a few months later, can be characterized by the equilibrium reached ultimately between the free troposphere and the regional oceans in the remote tropics, resulting in warmer regional SST. One of the outcomes is the increase in low-level atmospheric moisture and associated MSE from higher SST. We

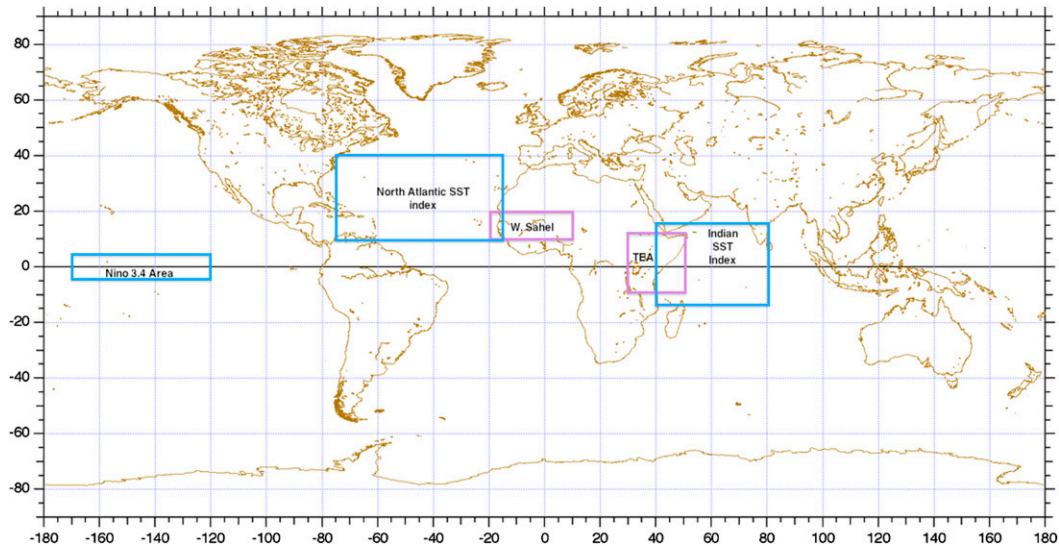


FIG. 2. Map showing the two relevant remote tropical land regions [western Sahel (10°S – 20°N , 20°W – 10°E) and tropical eastern Africa (10°S – 12°N , 30° – 52°E)] and their corresponding neighboring oceans [North Atlantic (10° – 40°N , 75° – 15°W) and Indian Ocean (15°S – 15°N , 40° – 80°E)] over which SSTs were averaged. Niño-3.4 region (5°S – 5°N , 170° – 120°W) is also shown.

hypothesize and test that a similar response should also be observed in those remote tropical land regions where the rainfall variability is driven by SSTs in the corresponding neighboring remote tropical oceans and ENSO region. Thus, the main expected characteristics of the mature phase for our remote tropical land region can be summarized as follows: (i) regional SST warming in the remote tropics, (ii) positive atmospheric CWV anomaly over the remote land region due to positive atmospheric CWV anomaly over the neighboring moisture source ocean region, and (iii) higher atmospheric instability over the remote land region from the bottom up in terms of positive upward vertical pressure velocity anomaly, resulting in (iv) enhancement of moist convection if higher MSE successfully breaks higher convective inhibition (D'Andrea et al. 2014; Gentine et al. 2013a,b). The likelihood of the number of times the low-level moisture and associated MSE overcomes the upped ante should then increase since low-level atmospheric moisture increases. This would suggest that we should see an increase (decrease) in number of wet (dry) days in terms of frequency and an increase in aggregated seasonal accumulation or mean. Despite the upped ante and higher low-level MSE, the response of extreme rainfall intensity is not clear since the MSE accumulation or dissipation process is not straightforward.

We chose two climatologically homogenous regions (see Fig. 2) over tropical Africa, the western Sahel (10° – 20°N , 20°W – 10°E) and tropical eastern Africa (10°S – 12°N , 30° – 52°E), as promising candidates to illustrate our proposed hypothesis for two reasons. First, variability of seasonal rainfall over these two regions is known to be

affected by ENSO (Giannini et al. 2008; Indeje et al. 2000; Janicot et al. 1996; Ropelewski and Halpert 1987; Ward 1998) and by SST in the regional neighboring ocean. Giannini et al. (2013) and Goddard and Graham (1999) identified North Atlantic SST (relative to global tropical SST) and Indian Ocean SST as the main driver of variability in rainfall characteristics over the western Sahel and TEA, respectively. Second, the corresponding rainy seasons (JAS and OND) coincide with our hypothesized growth and mature phases of El Niño, respectively. Evidence for our assertion that the JAS and OND seasons coincide with the growth and mature phases of El Niño evolution over the western Sahel or the neighboring North Atlantic Ocean and TEA or the neighboring Indian Ocean, respectively, is provided in section 4.

Thus, the two hypotheses that we explore through data analysis are as follows:

- 1) Since the JAS rainy season over the western Sahel coincides with the growth phase of El Niño evolution, the convective suppression or drier type of climate should be the response.
- 2) As the OND short rainy season over TEA coincides with the mature phase of El Niño evolution, the moist convective enhancement or wetter type of climate should be the outcome.

3. Datasets and methods

Daily rainfall data from 1979 to 2013 (35 years) with $0.5^{\circ} \times 0.5^{\circ}$ spatial resolution were taken from a surface

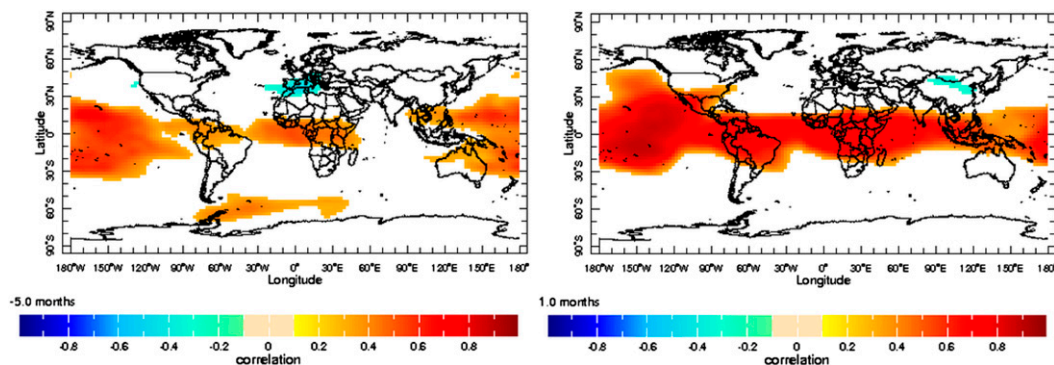


FIG. 3. Correlation maps of the monthly upper-tropospheric temperature (200-hPa level) with peak Niño-3.4 at different lag and lead times showing for (left) June prior to El Niño's peak, -5 -month lag with peak Niño-3.4 lagging TT and (right) December, $+1$ -month lead with peak Niño-3.4 leading TT. Data are over the period 1949–2013. Only significant correlation values are plotted in color. The 1% significance level is approximately 0.3 for time series of 65 yr.

rain gauge–derived global gridded product by the National Oceanic and Atmospheric Administration (NOAA)/Climate Prediction Center (CPC) (Chen et al. 2008; Xie et al. 2007). For the western Sahel and TEA, there are $60 \times 20 = 1200$ and $44 \times 44 = 1936$ grid boxes, respectively. The analyses of daily rainfall were also repeated (not reported here) with recent satellite retrievals and gauge data merged Africa rainfall climatology version 2 dataset (ARC2; Novella and Thiaw 2013), obtaining similar results as with the CPC gauge-based dataset.

Monthly SST and Niño-3.4 index data came from Kaplan et al. 1998. El Niño, La Niña, and neutral years were classified based on the condition that the running average of July–December (JASON) SST anomaly over the Niño-3.4 region be greater than 0.4°C , less than -0.4°C , or between -0.4° and 0.4°C , respectively. This ENSO classification is based on the canonical definition in Trenberth (1997). Note that the Niño-3.4 region extends from 170° to 120°W and from 5°S to 5°N (see Fig. 2).

Observed daily CWV, vertical pressure velocity, and TT (at 200-hPa level) data were taken with $2.5^{\circ} \times 2.5^{\circ}$ spatial resolution from the National Centers for Environmental Prediction–National Center for Atmospheric Research reanalysis dataset (Reanalysis-1; Kalnay et al. 1996). The analyses were also repeated for daily CWV and vertical pressure velocity (not reported here) with the Reanalysis-2 dataset (Kanamitsu et al. 2002), and similar results were obtained as with the Reanalysis-1 data.

To construct the empirical distributions, observed or reanalysis gridded daily samples of rainfall, CWV, and vertical pressure velocity were taken for all the grid boxes falling under the corresponding relevant land and ocean regions (as shown in Fig. 2). The empirical probability density functions of daily rainfall, CWV, and vertical pressure velocity were constructed by applying

the nonparametric Kernel density estimation using the “Gaussian kernel” (Sheather 1991) separately for El Niño, La Niña, and neutral years. The distributions for the different ENSO phases were compared using a nonparametric two-sample Kolmogorov–Smirnov (K-S) test (Marsaglia et al. 2003). Since CWV and vertical pressure velocity values exceeding higher-percentile values are important for deep moist convective events, values exceeding a conservative 50th-percentile threshold were taken (of all daily values during the rainy seasons across 35 years for all grid points over each focus region). Note that the empirical distributions for the La Niña years are shown for reference, but the focus here is on the comparison of El Niño and neutral years.

4. TT and SST evolution during El Niño

We first analyze and discuss the fast and slow evolution of tropical TT and SST, respectively, relative to El Niño development to justify the assumptions that the JAS and OND seasons coincide with the growth and mature phases of El Niño over the western Sahel and neighboring North Atlantic Ocean and over TEA and the neighboring Indian Ocean, respectively. In Figs. 3 and 4 we plot maps of TT (at 200-hPa level) and SST evolution during ENSO, represented by their lag–lead correlations with peak Niño-3.4, defined as the average of November and December values.

As per our growth and mature phase hypotheses, we expect to see a fast and uniform response in TT and a delayed response in SST, respectively. Figure 3 (left) shows that in the very early part of the growth phase in June prior to El Niño peak (-5 -month lag, with peak Niño-3.4 lagging TT), the TT signal has already reached the tropical Atlantic Ocean and Africa. By the end of

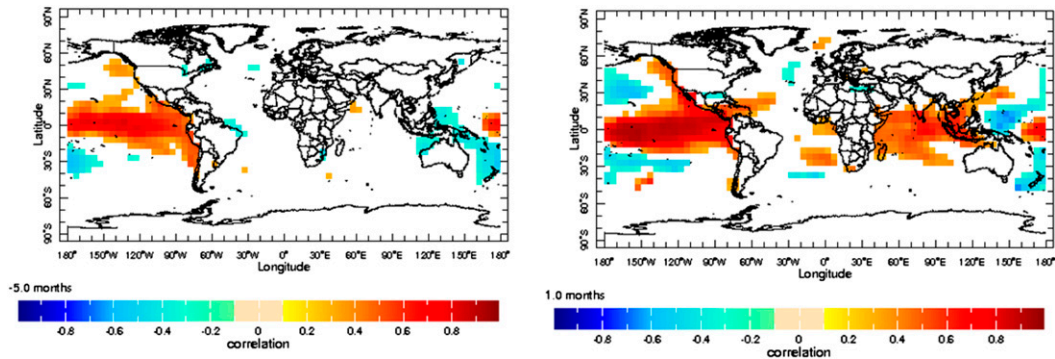


FIG. 4. Correlation maps of monthly SST with peak Niño-3.4 at different lag and lead times showing for (left) June prior to El Niño's peak, -5 -month lag with peak Niño-3.4 lagging SST and (right) December, $+1$ -month lead with peak Niño-3.4 leading SST. Data are over the period 1949–2013. Only significant correlation values are plotted in color. The 1% significance level is approximately 0.3 for time series of 65 yr.

the mature phase, in December ($+1$ -month lead, with Niño-3.4 leading TT; see Fig. 3, right), the TT has responded uniformly across the whole tropical zone including over the Indian Ocean. Figure 4 shows the delayed response in SST as discussed next.

Figure 4, left, shows that there is no significant correlation between peak Niño-3.4 and monthly SST in the equatorial or North Atlantic in June prior to El Niño peak (-5 -month lag, with peak Niño-3.4 lagging SST), during what we call the growth phase. This confirms that the North Atlantic SST has not adjusted to the TT warming during the western Sahel rainy season (JAS), supporting our growth phase hypothesis.

In contrast to the lack of North Atlantic SST response during the growth phase, there is significant correlation between peak Niño-3.4 and monthly SST in the Indian Ocean during what we call the mature phase (October–December), as shown in the correlation map in Fig. 4, right (for December, $+1$ -month lead, with Niño-3.4 leading SST). This confirms that the Indian Ocean SST has adjusted to the TT warming during the TEA short rainy season (OND), supporting our El Niño teleconnection mature phase hypothesis.

5. Rainfall analysis

We next analyze the modulation in total seasonal rainfall as well as its daily frequency and intensity behavior associated with the ENSO teleconnection. We expect to see suppression and enhancement in moist convective activity manifested through changes in frequency and/or intensity over the western Sahel and TEA, respectively.

Before analyzing the modulation in different characteristics of rainfall, we tested if the daily rainfall response to El Niño-related warming is robust for the rainfall distribution across ENSO phases. Nonparametric empirical

distributions of daily rainfall were constructed for El Niño, La Niña, and neutral years and compared using a two-sample Kolmogorov–Smirnov test. The K-S test asks how likely it is that the groups in each comparison came from the same distribution. K-S tests indicated that the empirical distributions for El Niño versus neutral years are significantly different at the 1% level. We then analyzed seasonal total or mean amount, frequency of wet days, and daily intensity values [for days where rainfall $> 1 \text{ mm day}^{-1}$; such as mean, median, and extreme (99.9th percentile)] to understand the detailed characteristics of change in rainfall behavior.

Before delving into the details of the rainfall analyses, we first summarize the salient findings and confirm that they were in line with expectations from El Niño teleconnection growth and mature phase hypotheses:

- 1) There is a significant but opposite modulation in seasonal amount over western Sahel and TEA, which may be explained by the change in the number of wet days (Moron et al. 2007).
- 2) There is also a significant and opposite change in the number of wet days over the western Sahel and TEA.
- 3) However, there is no significant modification in the mean, median, or extreme daily rainfall intensity over both land regions.

a. Seasonal amount

Figure 5 shows the scatterplots of seasonal mean rainfall conditional on the JASON Niño-3.4 and regional SST indices. The regional SST indices represent the remote tropical ocean regions acting as the moisture source for the rainfall over the relevant remote tropical land regions. There is significant interannual variability in the seasonal mean of daily rainfall over the western Sahel and TEA with ENSO since the linear

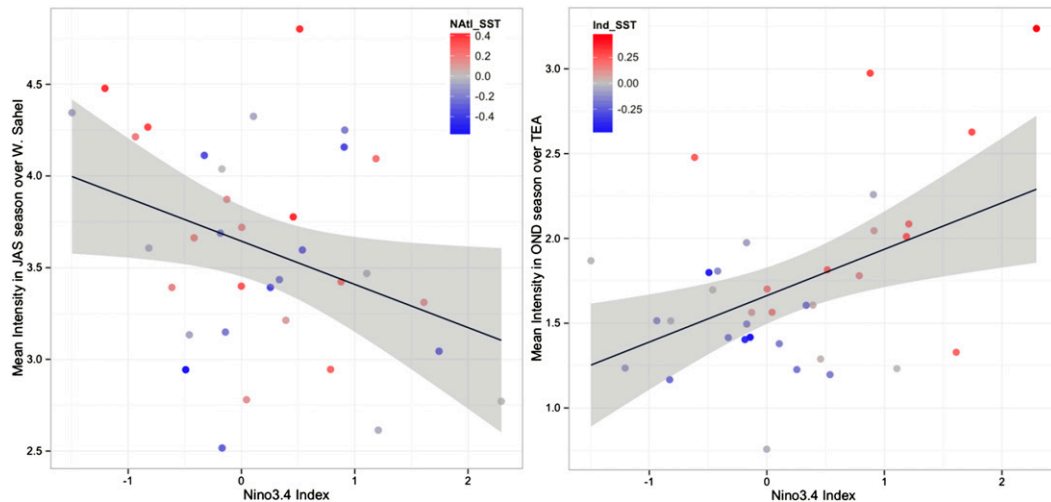


FIG. 5. Scatterplot of seasonal mean of all daily rainfall (mm day^{-1}), including dry days, on the y axis for (left) western Sahel during the JAS season and (right) TEA during the OND season, conditional on the Niño-3.4 index (x axis). The color of the circles indicates the normalized regional SST anomaly of the neighboring North Atlantic and Indian Oceans, respectively, with color fading from dark red to gray to dark blue corresponding to warmest to neutral to coolest normalized regional SST. The black line is a linear fit (mean vs Niño-3.4) with gray shading showing the 95% confidence band. Both regression fits are significant at the 5% level. The R^2 and p values of the slopes are 12% and 0.03, respectively, for western Sahel and 20% and 0.006, respectively, for TEA.

regression slopes are significant at the 5% level. This is in line with findings from prior studies (Janicot et al. 2001; Nicholson and Kim 1997; Rowell 2001), which considered observed data at the monthly time scale.

The normalized regional SST anomaly in the remote tropics (represented by the color of the dots, fading from dark red to gray to dark blue corresponding to warmest to neutral to coolest SST) is also shown in the figure (Fig. 5). The plots highlight how in the case of the western Sahel, the regional North Atlantic SST does not consistently warm with El Niño (red points are scattered on both left or right sides in Fig. 5, left, and the North Atlantic SST–Niño-3.4 Spearman rank correlation of -0.08 is not significant at the 1% level), while in the case of TEA, the Indian Ocean warms consistently (more red points toward the right in Fig. 5, right, and the Indian Ocean SST–Niño-3.4 Spearman rank correlation of 0.58 is significant at the 1% level).

b. Frequency: Number of wet days

The frequency of wet days during the rainy season (in terms of percentage of days with rainfall exceeding 1 mm day^{-1}) conditional on ENSO strength, as measured by the JASON Niño-3.4 index on the x axis, is shown in Fig. 6. The number of wet days is suppressed (significant downward linear trend at the 5% significance level in Fig. 6, left) and enhanced (significant upward linear trend at the 1% significance level in Fig. 6, right) over the western Sahel and TEA, respectively.

Additionally, we suggest that the variability in the seasonal amount is explained by the variability in the number of wet days since the nonparametric Spearman rank correlation is significant between seasonal mean rainfall and number of wet days (0.73 for western Sahel and 0.67 for TEA, both significant at the 1% level).

c. Intensity: Mean, median, and extreme rainfall

To check if the intensity of mean or any particular daily rainfall percentile is sensitive to ENSO, we constructed indices for the mean, median (50th percentile), and extreme intensity (99.9th percentile) derived with wet days only (rainfall $> 1 \text{ mm day}^{-1}$) and conducted linear regression analysis with our ENSO index.

We found that for mean daily intensity (for rainfall $> 1 \text{ mm day}^{-1}$), there is no significant variability with ENSO over the western Sahel and TEA. The linear regression slopes are not significant at the 10% level (p values are 0.22 and 0.30 for western Sahel and TEA, respectively). This further confirms that the seasonal mean or total amount (derived from all days including dry or no rainy days) is primarily modulated by the number of wet days (i.e., frequency of daily rainfall) rather than by the rainfall intensity, since both seasonal mean or total amount and frequency of wet days show significant covariability as discussed in section 5b.

Moreover, as in the case of mean daily intensity, the linear regressions indicate no significant modulation with ENSO for the median and extreme intensity (see

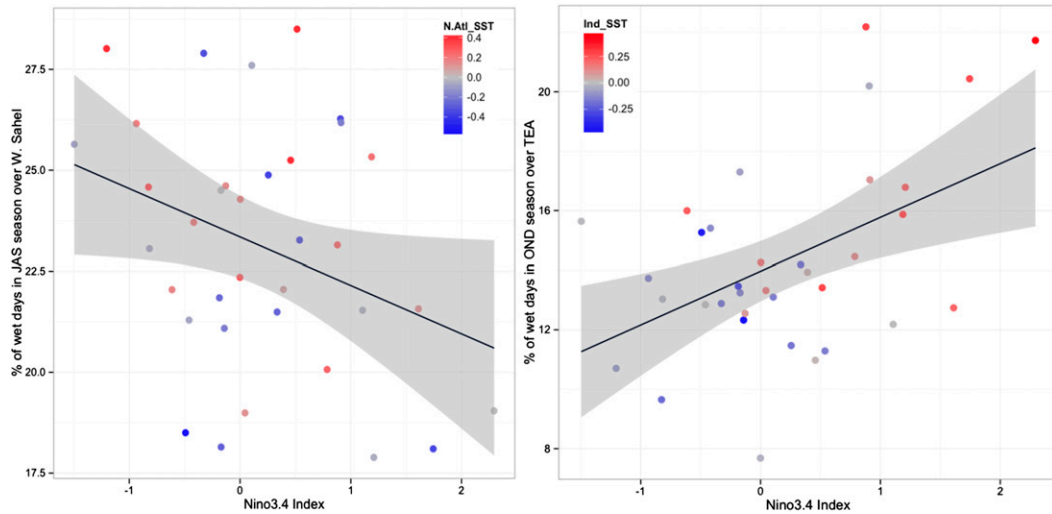


FIG. 6. As in Fig. 5, but for percent of wet days ($>1 \text{ mm day}^{-1}$) in the respective rainy season on the y axis for (left) western Sahel during the JAS season and (right) TEA during the OND season, conditional on the Niño-3.4 index (x axis). Both regression fits are significant at the 5% level. The R^2 and p values of the slopes are 11% and 0.04, respectively, for western Sahel and 23% and 0.003, respectively, for TEA.

Figs. 7 and 8). However, qualitatively, the modulation trend of median and extreme rainfall with ENSO is of similar sign (negative over western Sahel and positive over TEA) to that of the number of wet days or mean rainfall, with one exception. The modulation in extreme rainfall over the western Sahel shows a small (not significant) positive trend (Fig. 8, left). This could be due to the higher moisture and associated MSE buildup during El Niño years, when the number of deep convective

events or wet days is less as a result of higher atmospheric stability. We note that most extreme rainfall events are associated with a mesoscale convective system (MCS) induced by African easterly waves (AEW) over the Sahel (Mathon et al. 2002) and that AEW strength has been associated with ENSO (Okonkwo 2014). Since there is a lot of scatter in the median and extreme rainfall intensities and the regression lines are not significant, we refrain from concluding on the

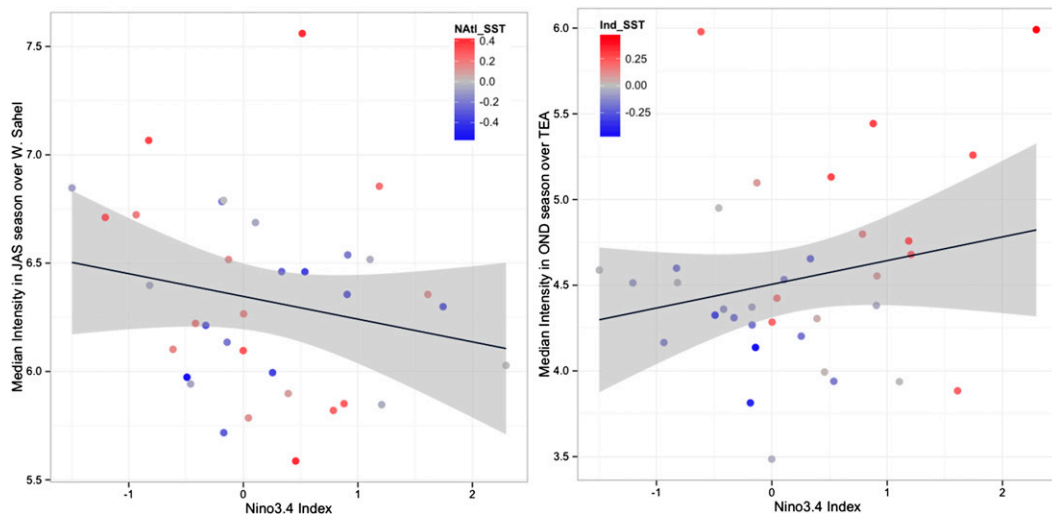


FIG. 7. As in Fig. 5, but for median rainfall intensity on the y axis (only for rainfall $>1 \text{ mm day}^{-1}$) for (left) western Sahel during the JAS season and (right) TEA during the OND season. Neither regression fits is significant. The R^2 and p values of the slopes are 4.29% and 0.23, respectively, for western Sahel and 4.5% and 0.21, respectively, for TEA.

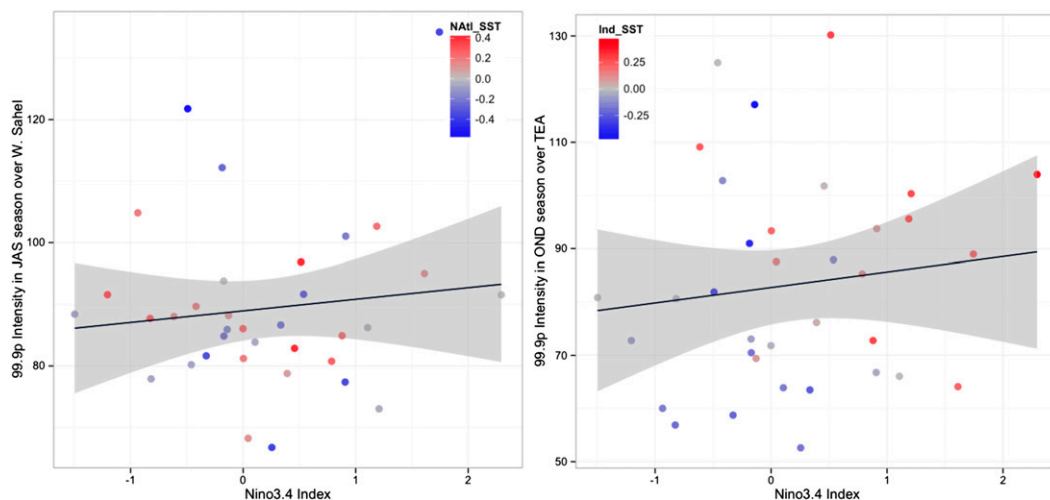


FIG. 8. As in Fig. 5, but for extreme (99.9th percentile) rainfall intensity on the y axis (only for rainfall $> 1 \text{ mm day}^{-1}$) of daily rainfall for (left) western Sahel during the JAS season and (right) TEA during the OND season. Neither regression fits are significant at the 5% level. The R^2 and p values of the slope are 1.4% and 0.498, respectively, for western Sahel and 1.6% and 0.468, respectively, for TEA. Note that for each year our sample size is 110 400 and 178 112 over the western Sahel and TEA, respectively.

modulation, except to say that the median or extreme rainfall events do not appear to be suppressed or enhanced over the western Sahel and TEA, respectively, unlike the seasonal mean rainfall and number of wet days.

6. Analysis of column water vapor

Next we analyze precipitable water through CWV, which is a proxy for moisture availability and a more homogenous field than rainfall (Holloway and Neelin 2010). First, we summarize our main findings from the CWV analysis as follows: 1) during the JAS season of El Niño years (prior to El Niño peak), an anomalous moisture condition relative to that during neutral years does not occur over the North Atlantic and the western Sahel, in line with the expectation from our growth phase hypothesis; and 2) during the OND season of El Niño years, positive moisture anomalies do occur relative to neutral years over the Indian Ocean and TEA, as expected from our mature phase hypothesis.

We showed in Fig. 4 that regional North Atlantic JAS season SSTs do not warm anomalously during El Niño years and, therefore, that no positive low-level moisture or MSE anomaly and subsequent CWV anomaly should occur over the North Atlantic. Figure 9 (left) shows that, during the JAS season over the North Atlantic, El Niño and neutral years have similar CWV probability distributions. Since the JAS rainy season is characterized by low-level onshore flow from the North Atlantic (Lu 2009), no positive CWV anomaly is expected over the western Sahel. This is confirmed to be the

case in Fig. 10, left. Comparing the empirical distribution of daily CWV composites over the western Sahel (Fig. 10, left) and applying a nonparametric K-S test, we find that the distributions of El Niño (shown in red solid line) and neutral years (shown in gray dotted line) are not significantly different (10% significance level). This suggests that an anomalous moisture condition over the western Sahel does not occur during El Niño years, in line with expectation from our growth phase hypothesis. Thus, we can infer that the reduction in the number of wet days is mainly driven by an increase in atmospheric stability caused by TT warming rather than as a result of any change in low-level moisture or MSE.

In contrast, we showed that the neighboring regional Indian Ocean OND season SSTs warm anomalously during El Niño years (significant positive correlation with ENSO SST index; see Fig. 4) and, therefore, that positive moisture or MSE anomalies and subsequent CWV anomalies should be observed over the Indian Ocean. Figure 9 (right) shows that during the OND season over the Indian Ocean during El Niño years the CWV probability distribution shifts toward higher values relative to neutral years [higher values are critical for deep convection as per Peters and Neelin (2006)]. Since the OND short rainy season over TEA is characterized by low-level onshore flow from the Indian Ocean (Goddard and Graham 1999), positive CWV anomalies are expected over TEA during El Niño years relative to neutral years. Comparing composites of the distributions of CWV over TEA (Fig. 10, right) and applying the K-S test, we find that the distribution composites of El

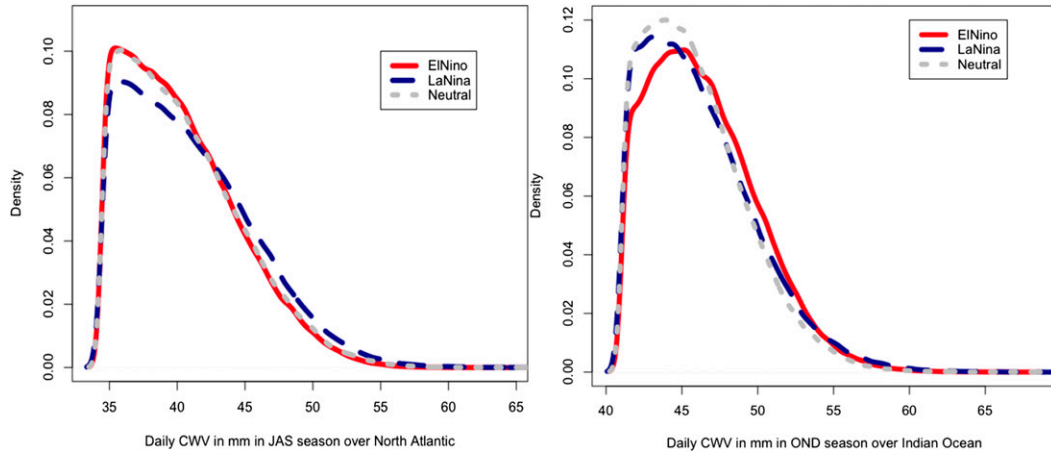


FIG. 9. Empirical distribution of daily CWV (mm) composited for El Niño (red solid), La Niña (blue dashed), and neutral (gray dotted) years for (left) North Atlantic Ocean during the JAS season and (right) Indian Ocean during the OND season. Values exceeding a fixed 50th percentile of all daily CWV values were taken.

Niño and neutral years are significantly different at the 1% level. Furthermore, the probability distribution of El Niño years is wider than that of neutral years for higher percentiles (see Fig. 10, right), which confirms that high anomalous moisture conditions over TEA occur during El Niño years, as expected from our mature phase hypothesis. Thus, the increase in the number of wet days (shown in the rainfall analysis section) is likely fueled by an increase in moisture convergence. However, dynamical reasons also contribute to such enhancement of rainfall. We report on these in the next section.

7. Analysis of vertical pressure velocity

We analyze midtropospheric (500 mb; 1 mb = 1 hPa) vertical pressure velocity (ω), which reflects stability or

instability of the atmosphere in deep moist convective events. During deep moist convection, vertical motions resulting from thermally driven turbulent mixing take parcels from the lower atmosphere to above the 500-mb level. Vertical pressure velocities exceeding higher-percentile values are associated with deep moist convective events. Thus, we took values less than a conservative 50th-percentile threshold of all daily values in the rainy season across 35 years for all grid points over each focus region—we note that the negative values of pressure velocity represent rising motions.

We first summarize our main findings from the analysis of ω as follows:

- 1) Anomalously more stable conditions over the western Sahel during the JAS season occur during El

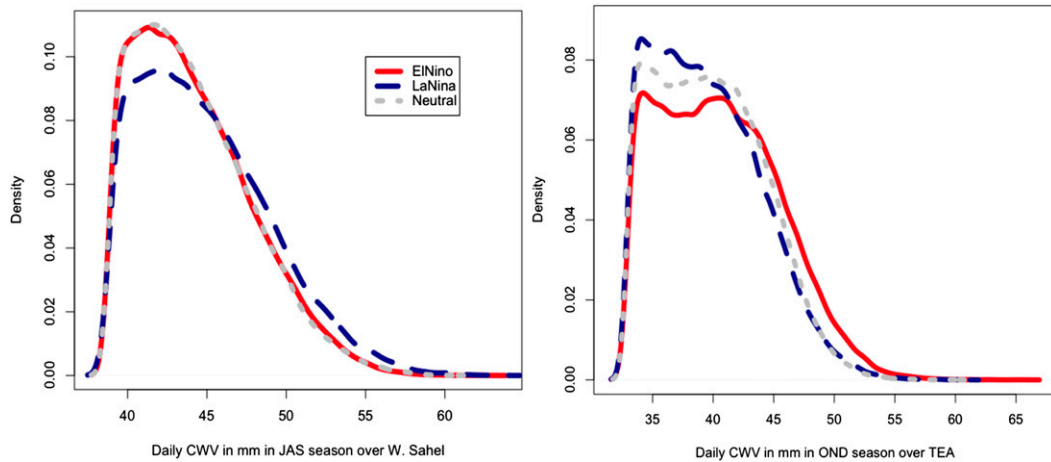


FIG. 10. As in Fig. 9, but for over remote tropical land regions: (left) western Sahel during the JAS season and (right) TEA during the OND season. Values exceeding a fixed 50th percentile of all daily CWV values were taken.

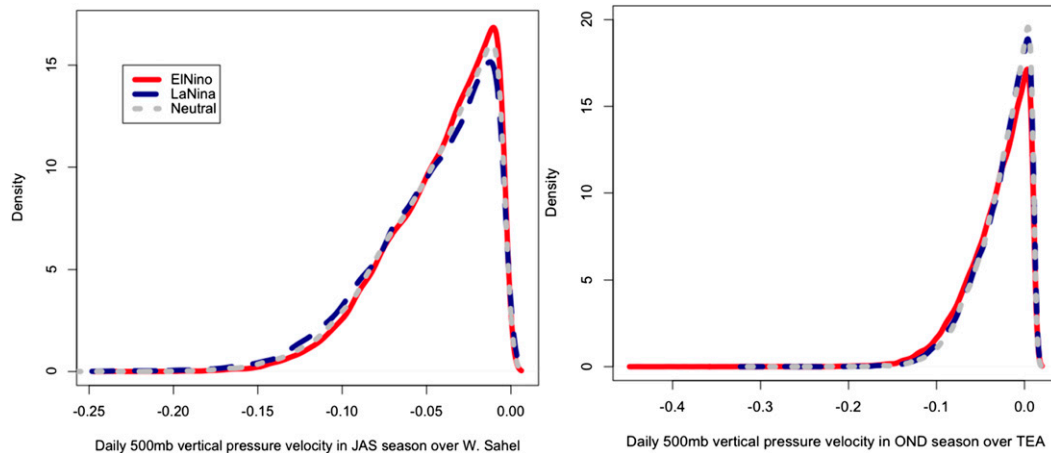


FIG. 11. As in Fig. 9, but for upward vertical pressure velocity at 500-mb level over (left) the western Sahel during the JAS season and (right) TEA during the OND season. Values exceeding a fixed 50th percentile threshold of all daily vertical 500-mb pressure velocity values were taken.

Niño years relative to neutral years, in line with expectation from our growth phase hypothesis. This suggests that the suppression in the number of wet days over the western Sahel during the JAS season is driven by higher atmospheric stability introduced from the top by TT warming since we already showed that there is no anomalous moisture anomaly.

- 2) An anomalously more unstable condition over TEA occurs during El Niño years relative to neutral years, as expected from our mature phase hypothesis. This confirms that the enhancement in the number of wet days over TEA during the OND season can be understood as the low-level moisture and associated MSE convergence exceeding the upped ante introduced by the high-level TT warming.

In the western Sahel, upper-tropospheric warming causes a more stable atmospheric profile driven from the top. This coincides with the lack of anomalous moisture, as shown in the last section, failing to destabilize the atmosphere from the bottom up. Stronger stability should be observed in terms of a significant difference between the distribution of ω during El Niño and neutral regimes and neutral year probability density exceeding that of El Niño years for higher percentiles. Comparing the nonparametric distribution composites of ω at the 500-mb level over the western Sahel (see Fig. 11, left) and applying the K-S test, we find that the distributions of El Niño and neutral years are indeed significantly different at 1% level and that the probability densities for higher percentiles during neutral years exceed those during El Niño years.

The dynamical analysis of the response of the mature phase hypothesis over TEA is more complex. Upper-tropospheric warming, acting from the top

down, tends to stabilize the atmosphere by creating an upped ante, while anomalously higher moisture in the ABL acting from the bottom tries to catch up with the upped ante. When the positive anomaly in low-level moisture and associated MSE exceeds the anomalous stability imposed from the top by tropospheric warming, the atmosphere ultimately destabilizes. This behavior should be reflected in significant differences between the distribution of ω during El Niño and neutral regimes and in wider probability densities during El Niño years for higher percentiles relative to neutral years. Based on comparison of the nonparametric distribution composites of ω and on application of the K-S test, we find that the upper-tail probability (for higher percentiles) during El Niño years indeed exceeds that of neutral years (see Fig. 11, right) and that the distributions of El Niño and neutral years are significantly different at the 1% level, indicating that the moisture or MSE dominates over the higher convective threshold or convective inhibition.

8. Summary and discussion

a. Summary

We summarize our main findings and conclusions here.

- This observational study provides evidence for the contrasted modulation in regional rainfall over remote tropical land by the tropical tropospheric temperature mechanism during El Niño years.
- Over the western Sahel, the El Niño teleconnection is primarily associated with the decrease in seasonal mean rainfall (section 5a; Fig. 5, left) and decrease in the number of wet days (section 5b; Fig. 6, left), in line

with expectation from the growth phase hypothesis. The decrease in number of wet days in turn explains the decrease in the seasonal mean rainfall over the western Sahel.

- Over TEA, the El Niño teleconnection is associated with an increase in seasonal mean rainfall (section 5a; Fig. 5, right) and an increase in the number of wet days (section 5b; Fig. 6, right), as expected from the mature phase hypothesis. Furthermore, the increase in number of wet days explains the increase in the seasonal mean rainfall over TEA.
- Unlike the frequency of wet days or seasonal mean (or total) rainfall, daily mean, median, and extreme (99.9th percentile) rainfall intensities (rainfall > 1 mm day⁻¹) are not modulated (section 5c) over both the western Sahel (Figs. 7 and 8, left) and TEA (Figs. 7 and 8, right), meaning that during an El Niño year, a daily extreme rainfall event can still occur in the western Sahel.

Qualitatively, our findings are consistent with Rodríguez-Fonseca et al. (2011), who highlight that SST anomalies in the equatorial Atlantic and Pacific tend to have opposite sign of influence on Sahel rainfall. Furthermore, Mohino et al. (2011) showed that the interannual variability of Sahel rainfall is affected by SST anomalies in all ocean basins. Further, Giannini et al. (2013) explained the changes in rainfall characteristics over the Sahel with the relative warming of the neighboring regional ocean (North Atlantic) with respect to the global tropical oceans. We corroborate these findings and further suggest that the SST in the regional ocean's influence on the neighboring land will be in contrast to the aggregated tropical zonal SSTs in other ocean basins—particularly dominated by the tropical Pacific Ocean.

b. Discussion

Land–atmospheric feedbacks could play an important role in modulating rainfall variability since land can also carry one or two months of memory through soil moisture and vegetation, particularly over semiarid regions such as the western Sahel (Koster and Suarez 2001; Zeng et al. 1999; Lee et al. 2012). In addition to or in the absence of soil moisture, anomalous circulations triggered by spatial gradients of moisture and temperature fields between land and ocean or ocean and ocean can further create convergence of moisture over land. However, we have chosen our land regions and seasons such that the variability of rainfall is primarily driven by changes in SSTs over the regional neighboring ocean and tropical Pacific (ENSO region). Thus, ignoring specific complexities of the land surface (e.g., soil moisture) should

not affect our analysis, at least qualitatively. Furthermore, as in Tang and Neelin (2004), residual warming of the North Atlantic Ocean the year after an El Niño event due to equilibrated SST (mature phase behavior) could provide higher moisture supply and cause more wet days over the western Sahel. The Madden–Julian oscillation (MJO) is also known to modulate rainfall at the intraseasonal time scale over both the western Sahel (Lavender and Matthews 2009) and TEA (Berhane and Zaitchik 2014; Pohl and Camberlin 2006) and could be another potential reason for more scatter, since MJO events show variability and in general are more active during ENSO neutral years. Yet one more potential source of scatter over the western Sahel could be understood by the rate at which TT warming evolves, as suggested by Chiang and Sobel (2002). A faster (slower) change in TT warming brings more (less) disequilibrium with stronger (weaker) rainfall response.

The magnitude of the surface fluxes from different sources in the air–sea interaction are difficult to quantify and will be decided ultimately by more accurate surface flux measurements. One study (Tsintikidis and Zhang 1998) suggests that at lower SST (less than ~301 K), change in surface evaporation is dominantly explained by temperature and moisture effects and at higher SST (greater than ~301 K) by wind speed. During our study period (1979–2013), we find that JAS seasonal average SST over our North Atlantic box was less than about 301 K, and that for the OND season over the Indian Ocean box was sometimes above about 301 K but was always below about 301.5 K. This suggests that the TT mechanisms acting through the air–sea exchange of temperature and moisture fluxes also contribute in maintaining the SST–MSE coupling (CS02; Saravanan and Chang 2000) along with other mechanisms such as surface wind or cloud radiative fluxes.

Our mature phase hypothesis does not necessarily dictate that the rainfall response will be anomalously wet in all tropical land regions remote from the tropical Pacific basin. The stability induced from the top by TT warming still continues during the mature phase, and only if moisture convergence is sufficient to destabilize the atmospheric column from the bottom can a wet anomaly response emerge. It is also possible that, because of other local factors such as delay in warming of the SST in the moisture source region, sufficient moisture advection and convergence do not occur, resulting in an anomalously dry rainfall response. Thus, while the dry response of rainfall in southern Africa during the mature phase of El Niño may seem at first glance puzzling, there are reasons why this situation is less pertinent to our mature phase hypothesis: (i) South Africa's climate is influenced by both tropical and extratropical

dynamics complicating the analysis, as highlighted by Cook et al. (2006) and Lyon and Mason (2007)—for example, cold fronts influence the southwest winter rainfall (Reason and Rouault 2002); and (ii) delay in warming of the South Atlantic region (see Fig. 4) as a potential moisture source.

Finally, a caveat is that the modulation of convective events or wet days as described in the paper during the growth or mature phase of El Niño evolution is mainly applicable over precipitating regions and seasons. Thus, it might be interesting to investigate if the TT mechanism under growth and mature hypotheses can explain the modulation in rainfall in other remote tropical land regions, such as India (JAS rainy season) and Sri Lanka (OND rainy season). In nonprecipitating regions, the surface response is expected to be weaker, since deep moist convection provides the strongest link between the ABL and free troposphere.

c. Implication for global warming

In the case of GW, warming of the local or regional neighboring ocean provides the lower-level instability through onshore moisture or MSE advection, while the average global tropical ocean warming sets the threshold for the atmospheric stability from the top through a uniform warming of the tropical free troposphere. If GW manifests as slower warming of the regional ocean acting as the moisture source for the remote tropical land relative to the average global tropical oceans, it can be considered analogous to our disequilibrium or growth phase ENSO teleconnection hypothesis. The outcome would then be an increase in stability of the troposphere without sufficient moisture convergence, resulting in suppression of the number of wet days and mean rainfall over those land regions whose rainfall is primarily driven by onshore moisture advection (usually monsoon regions). On the other hand, if GW were to manifest in terms of the regional ocean (moisture source) warming similarly to or faster than the average of the global tropical oceans, it can be deemed analogous to our equilibrium or mature phase El Niño teleconnection hypothesis. Even if the upper-tropospheric warming continues to induce stability from the top, the net outcome will be destabilization of the atmosphere and an increase in the number of wet days and mean rainfall over the remote tropical land regions if sufficient moisture convergence breaks the higher convective barrier. These ideas are consistent with the “upped ante” and “rich gets richer” mechanisms proposed by Chou and Neelin (2004). CS02 showed that rainfall and SST responses increase and decrease, respectively, with an increased ocean mixed layer depth (MLD), where variations in MLD are used to “parameterize” the time scale of the adjustment of atmospheric boundary layer

and determine when a regional response might transition from a growth- or disequilibrium-type phase to a mature or equilibrium one.

It is not clear whether anthropogenic GW will result in increased response of the growth or mature type. Giannini et al. (2003) suggested that tropospheric stability was partly responsible for the Sahel drought during the 1970s and 1980s. Held et al. (2005) pointed out the lack of consensus in the Sahel rainfall response of coupled climate models under a simplified GW scenario. If in response to GW, SST patterns were to evolve similarly to an El Niño-type SST pattern (Meehl and Washington 1996; Song and Zhang 2014; Teng et al. 2006; Yeh et al. 2012), our findings would be relevant in interpreting the heterogeneous rainfall response.

There is considerable uncertainty in the spatial pattern of the evolution of SSTs under GW (Song and Zhang 2014). A few climate models indicate that SSTs under GW might manifest as a La Niña-like pattern (An et al. 2012; Liu et al. 2005). Thus, understanding the heterogeneous response of rainfall under La Niña would also be relevant, and our study can also be extended for such analysis. The response need not be linear since El Niño’s and La Niña’s spatial and temporal evolution over the tropical Pacific are asymmetric (Okumura and Deser 2010; Weller and Cai 2013).

Acknowledgments. Pradipta Parhi and Alessandra Giannini are supported by National Science Foundation Grant AGS-0955372. Pierre Gentine is supported by Department of Energy Grant DE-SC0011094 and NASA NIP 13-NIP13-0095. We thank the Columbia Water Center and Michael Bell of the International Research Institute for Climate and Society, Earth Institute at Columbia University, for providing support for resources and the datasets. We also thank three anonymous reviewers for their feedback.

REFERENCES

- Alexander, M. A., I. Bladé, M. Newman, J. R. Lanzante, N.-C. Lau, and J. D. Scott, 2002: The atmospheric bridge: The influence of ENSO teleconnections on air–sea interaction over the global oceans. *J. Climate*, **15**, 2205–2231, doi:10.1175/1520-0442(2002)015<2205:TABTIO>2.0.CO;2.
- An, S.-I., J.-W. Kim, S.-H. Im, B.-M. Kim, and J.-H. Park, 2012: Recent and future sea surface temperature trends in tropical Pacific warm pool and cold tongue regions. *Climate Dyn.*, **39**, 1373–1383, doi:10.1007/s00382-011-1129-7.
- Arakawa, A., and W. H. Schubert, 1974: Interaction of a cumulus cloud ensemble with the large-scale environment, part I. *J. Atmos. Sci.*, **31**, 674–701, doi:10.1175/1520-0469(1974)031<0674:IOACCE>2.0.CO;2.
- Berhane, F., and B. Zaitchik, 2014: Modulation of daily precipitation over East Africa by the Madden–Julian oscillation. *J. Climate*, **27**, 6016–6034, doi:10.1175/JCLI-D-13-00693.1.

- Camberlin, P., S. Janicot, and I. Poccard, 2001: Seasonality and atmospheric dynamics of the teleconnection between African rainfall and tropical sea-surface temperature: Atlantic vs. ENSO. *Int. J. Climatol.*, **21**, 973–1005, doi:10.1002/joc.673.
- Chen, M., W. Shi, P. Xie, V. B. S. Silva, V. E. Kousky, R. Wayne Higgins, and J. E. Janowiak, 2008: Assessing objective techniques for gauge-based analyses of global daily precipitation. *J. Geophys. Res.*, **113**, D04110, doi:10.1029/2007JD009132.
- Chiang, J. C. H., and A. H. Sobel, 2002: Tropical tropospheric temperature variations caused by ENSO and their influence on the remote tropical climate. *J. Climate*, **15**, 2616–2631, doi:10.1175/1520-0442(2002)015<2616:TTVCB>2.0.CO;2.
- , and B. R. Lintner, 2005: Mechanisms of remote tropical surface warming during El Niño. *J. Climate*, **18**, 4130–4149, doi:10.1175/JCLI3529.1.
- Chou, C., and J. D. Neelin, 2004: Mechanisms of global warming impacts on regional tropical precipitation. *J. Climate*, **17**, 2688–2701, doi:10.1175/1520-0442(2004)017<2688:MOGWIO>2.0.CO;2.
- Cook, B. I., G. B. Bonan, and S. Levis, 2006: Soil moisture feedbacks to precipitation in southern Africa. *J. Climate*, **19**, 4198–4206, doi:10.1175/JCLI3856.1.
- D'Andrea, F., P. Gentine, A. K. Betts, and B. R. Lintner, 2014: Triggering deep convection with a probabilistic plume model. *J. Atmos. Sci.*, **71**, 3881–3901, doi:10.1175/JAS-D-13-0340.1.
- Davey, M. K., A. Brookshaw, and S. Ineson, 2014: The probability of the impact of ENSO on precipitation and near-surface temperature. *Climate Risk Manage.*, **1**, 5–24, doi:10.1016/j.crm.2013.12.002.
- Emanuel, K. A., J. David Neelin, and C. S. Bretherton, 1994: On large-scale circulations in convecting atmospheres. *Quart. J. Roy. Meteor. Soc.*, **120**, 1111–1143, doi:10.1002/qj.49712051902.
- Fischer, E. M., U. Beyerle, and R. Knutti, 2013: Robust spatially aggregated projections of climate extremes. *Nat. Climate Change*, **3**, 1033–1038, doi:10.1038/nclimate2051.
- Gentine, P., A. K. Betts, B. R. Lintner, K. L. Findell, C. C. van Heerwaarden, and F. D'Andrea, 2013a: A probabilistic bulk model of coupled mixed layer and convection. Part II: Shallow convection case. *J. Atmos. Sci.*, **70**, 1557–1576, doi:10.1175/JAS-D-12-0146.1.
- , A. A. M. Holtslag, F. D'Andrea, and M. Ek, 2013b: Surface and atmospheric controls on the onset of moist convection over land. *J. Hydrometeorol.*, **14**, 1443–1462, doi:10.1175/JHM-D-12-0137.1.
- Giannini, A., R. Saravanan, and P. Chang, 2003: Oceanic forcing of Sahel rainfall on interannual to interdecadal time scales. *Science*, **302**, 1027–1030, doi:10.1126/science.1089357.
- , M. Biasutti, I. M. Held, and A. H. Sobel, 2008: A global perspective on African climate. *Climatic Change*, **90**, 359–383, doi:10.1007/s10584-008-9396-y.
- , S. Salack, T. Lodoun, A. Ali, A. T. Gaye, and O. Ndiaye, 2013: A unifying view of climate change in the Sahel linking intra-seasonal, interannual and longer time scales. *Environ. Res. Lett.*, **8**, 024010, doi:10.1088/1748-9326/8/2/024010.
- Goddard, L., and N. E. Graham, 1999: Importance of the Indian Ocean for simulating rainfall anomalies over eastern and southern Africa. *J. Geophys. Res.*, **104**, 19 099–19 116, doi:10.1029/1999JD900326.
- Goswami, B. N., and P. K. Xavier, 2005: ENSO control on the South Asian monsoon through the length of the rainy season. *Geophys. Res. Lett.*, **32**, L18717, doi:10.1029/2005GL023216.
- Hawkins, E., and R. Sutton, 2009: The potential to narrow uncertainty in regional climate predictions. *Bull. Amer. Meteor. Soc.*, **90**, 1095–1107, doi:10.1175/2009BAMS2607.1.
- Held, I. M., T. L. Delworth, J. Lu, K. L. Findell, and T. R. Knutson, 2005: Simulation of Sahel drought in the 20th and 21st centuries. *Proc. Natl. Acad. Sci. USA*, **102**, 17 891–17 896, doi:10.1073/pnas.0509057102.
- Herceg, D., A. H. Sobel, and L. Sun, 2007: Regional modeling of decadal rainfall variability over the Sahel. *Climate Dyn.*, **29**, 89–99, doi:10.1007/s00382-006-0218-5.
- Holloway, C. E., and J. D. Neelin, 2010: Temporal relations of column water vapor and tropical precipitation. *J. Atmos. Sci.*, **67**, 1091–1105, doi:10.1175/2009JAS3284.1.
- Indeje, M., F. H. M. Semazzi, and L. J. Ogallo, 2000: ENSO signals in East African rainfall seasons. *Int. J. Climatol.*, **20**, 19–46, doi:10.1002/(SICI)1097-0088(200001)20:1<19::AID-JOC449>3.0.CO;2-0.
- Janicot, S., V. Moron, and B. Fontaine, 1996: Sahel droughts and ENSO dynamics. *Geophys. Res. Lett.*, **23**, 515–518, doi:10.1029/96GL00246.
- , S. Trzaska, and I. Poccard, 2001: Summer Sahel-ENSO teleconnection and decadal time scale SST variations. *Climate Dyn.*, **18**, 303–320, doi:10.1007/s003820100172.
- Johnson, N. C., and S.-P. Xie, 2010: Changes in the sea surface temperature threshold for tropical convection. *Nat. Geosci.*, **3**, 842–845, doi:10.1038/ngeo1008.
- Kalnay, E., and Coauthors, 1996: The NCEP/NCAR 40-Year Reanalysis Project. *Bull. Amer. Meteor. Soc.*, **77**, 437–471, doi:10.1175/1520-0477(1996)077<0437:TNYRP>2.0.CO;2.
- Kanamitsu, M., W. Ebisuzaki, J. Woollen, S.-K. Yang, J. J. Hnilo, M. Fiorino, and G. L. Potter, 2002: NCEP–DOE AMIP-II Reanalysis (R-2). *Bull. Amer. Meteor. Soc.*, **83**, 1631–1643, doi:10.1175/BAMS-83-11-1631.
- Kaplan, A., M. A. Cane, Y. Kushnir, A. C. Clement, M. B. Blumenthal, and B. Rajagopalan, 1998: Analyses of global sea surface temperature 1856–1991. *J. Geophys. Res.*, **103**, 18 567–18 589, doi:10.1029/97JC01736.
- Klein, S. A., B. J. Soden, and N.-C. Lau, 1999: Remote sea surface temperature variations during ENSO: Evidence for a tropical atmospheric bridge. *J. Climate*, **12**, 917–932, doi:10.1175/1520-0442(1999)012<0917:RSSTVD>2.0.CO;2.
- Koster, R. D., and M. J. Suarez, 2001: Soil moisture memory in climate models. *J. Hydrometeorol.*, **2**, 558–570, doi:10.1175/1525-7541(2001)002<0558:SMMICM>2.0.CO;2.
- Lavender, S. L., and A. J. Matthews, 2009: Response of the West African monsoon to the Madden–Julian oscillation. *J. Climate*, **22**, 4097–4116, doi:10.1175/2009JCLI2773.1.
- Lee, J., and Coauthors, 2012: Reduction of tropical land region precipitation variability via transpiration. *Geophys. Res. Lett.*, **39**, L19704, doi:10.1029/2012GL053417.
- Liu, Z., S. Vavrus, F. He, N. Wen, and Y. Zhong, 2005: Rethinking tropical ocean response to global warming: The enhanced equatorial warming. *J. Climate*, **18**, 4684–4700, doi:10.1175/JCLI3579.1.
- Losada, T., B. Rodriguez-Fonseca, E. Mohino, J. Bader, S. Janicot, and C. R. Mechoso, 2012: Tropical SST and Sahel rainfall: A non-stationary relationship. *Geophys. Res. Lett.*, **39**, L12705, doi:10.1029/2012GL052423.
- Lu, J., 2009: The dynamics of the Indian Ocean sea surface temperature forcing of Sahel drought. *Climate Dyn.*, **33**, 445–460, doi:10.1007/s00382-009-0596-6.
- Lyon, B., and A. G. Barnston, 2005: ENSO and the spatial extent of interannual precipitation extremes in tropical land areas. *J. Climate*, **18**, 5095–5109, doi:10.1175/JCLI3598.1.
- , and S. J. Mason, 2007: The 1997–98 summer rainfall season in southern Africa. Part I: Observations. *J. Climate*, **20**, 5134–5148, doi:10.1175/JCLI4225.1.

- Marsaglia, G., W. Tsang, and J. Wang, 2003: Evaluating Kolmogorov's distribution. *J. Stat. Software*, **8**, doi:10.18637/jss.v008.i18.
- Mathon, V., H. Laurent, and T. Lebel, 2002: Mesoscale convective system rainfall in the Sahel. *J. Appl. Meteor.*, **41**, 1081–1092, doi:10.1175/1520-0450(2002)041<1081:MCSRIT>2.0.CO;2.
- Meehl, G. A., and W. M. Washington, 1996: El Niño-like climate change in a model with increased atmospheric CO₂ concentrations. *Nature*, **382**, 56–60, doi:10.1038/382056a0.
- Mohino, E., B. Rodríguez-Fonseca, C. R. Mechoso, S. Gervois, P. Ruti, and F. Chauvin, 2011: Impacts of the tropical Pacific/Indian Oceans on the seasonal cycle of the West African monsoon. *J. Climate*, **24**, 3878–3891, doi:10.1175/2011JCLI3988.1.
- Moron, V., A. W. Robertson, M. N. Ward, and P. Camberlin, 2007: Spatial coherence of tropical rainfall at the regional scale. *J. Climate*, **20**, 5244–5263, doi:10.1175/2007JCLI1623.1.
- Neelin, J. D., C. Chou, and H. Su, 2003: Tropical drought regions in global warming and El Niño teleconnections. *Geophys. Res. Lett.*, **30**, 2275, doi:10.1029/2003GL018625.
- , O. Peters, J. W.-B. Lin, K. Hales, and C. E. Holloway, 2008: Rethinking convective quasi-equilibrium: Observational constraints for stochastic convective schemes in climate models. *Philos. Trans. Roy. Soc. London*, **366A**, 2581–2604, doi:10.1098/rsta.2008.0056.
- Nicholson, S. E., 2013: The West African Sahel: A review of recent studies on the rainfall regime and its interannual variability. *ISRN Meteorology*, **2013**, 453521, doi:10.1155/2013/453521.
- , and J. Kim, 1997: The relationship of the El Niño–Southern Oscillation to African rainfall. *Int. J. Climatol.*, **17**, 117–135, doi:10.1002/(SICI)1097-0088(199702)17:2<117::AID-JOC84>3.0.CO;2-O.
- Novella, N. S., and W. M. Thiaw, 2013: African rainfall climatology version 2 for famine early warning systems. *J. Appl. Meteor. Climatol.*, **52**, 588–606, doi:10.1175/JAMC-D-11-0238.1.
- O'Gorman, P. A., 2012: Sensitivity of tropical precipitation extremes to climate change. *Nat. Geosci.*, **5**, 697–700, doi:10.1038/ngeo1568.
- Okonkwo, C., 2014: An advanced review of the relationships between Sahel precipitation and climate indices: A wavelet approach. *Int. J. Atmos. Sci.*, **2014**, 759067, doi:10.1155/2014/759067.
- Okumura, Y. M., and C. Deser, 2010: Asymmetry in the duration of El Niño and La Niña. *J. Climate*, **23**, 5826–5843, doi:10.1175/2010JCLI3592.1.
- Paeth, H., and P. Friederichs, 2004: Seasonality and time scales in the relationship between global SST and African rainfall. *Climate Dyn.*, **23**, 815–837, doi:10.1007/s00382-004-0466-1.
- Peters, O., and J. D. Neelin, 2006: Critical phenomena in atmospheric precipitation. *Nat. Phys.*, **2**, 393–396, doi:10.1038/nphys314.
- Philippon, N., N. Martiny, P. Camberlin, M. T. Hoffman, and V. Gond, 2014: Timing and patterns of the ENSO signal in Africa over the last 30 years: Insights from normalized difference vegetation index data. *J. Climate*, **27**, 2509–2532, doi:10.1175/JCLI-D-13-00365.1.
- Pohl, B., and P. Camberlin, 2006: Influence of the Madden–Julian oscillation on East African rainfall. I: Intraseasonal variability and regional dependency. *Quart. J. Roy. Meteor. Soc.*, **132**, 2521–2539, doi:10.1256/qj.05.104.
- Polo, I., B. Rodríguez-Fonseca, T. Losada, and J. García-Serrano, 2008: Tropical Atlantic variability modes (1979–2002). Part I: Time-evolving SST modes related to West African rainfall. *J. Climate*, **21**, 6457–6475, doi:10.1175/2008JCLI2607.1.
- Rajagopalan, B., and P. Molnar, 2014: Combining regional moist static energy and ENSO for forecasting of early and late season Indian monsoon rainfall and its extremes. *Geophys. Res. Lett.*, **41**, 4323–4331, doi:10.1002/2014GL060429.
- Reason, C. J. C., and M. Rouault, 2002: ENSO-like decadal variability and South African rainfall. *Geophys. Res. Lett.*, **29**, 1638, doi:10.1029/2002GL014663.
- Rodríguez-Fonseca, B., and Coauthors, 2011: Interannual and decadal SST-forced responses of the West African monsoon. *Atmos. Sci. Lett.*, **12**, 67–74, doi:10.1002/asl.308.
- Ropelewski, C. F., and M. S. Halpert, 1987: Global and regional scale precipitation patterns associated with the El Niño/Southern Oscillation. *Mon. Wea. Rev.*, **115**, 1606–1626, doi:10.1175/1520-0493(1987)115<1606:GARSPP>2.0.CO;2.
- Rowell, D. P., 2001: Teleconnections between the tropical Pacific and the Sahel. *Quart. J. Roy. Meteor. Soc.*, **127**, 1683–1706, doi:10.1002/qj.49712757512.
- Saravanan, R., and P. Chang, 2000: Interaction between tropical Atlantic variability and El Niño–Southern Oscillation. *J. Climate*, **13**, 2177–2194, doi:10.1175/1520-0442(2000)013<2177:IBTAVA>2.0.CO;2.
- Sheather, S. J., 1991: A reliable data-based bandwidth selection method for kernel density estimation. *J. Roy. Stat. Soc.*, **53B**, 683–690.
- Sobel, A. H., J. Nilsson, and L. M. Polvani, 2001: The weak temperature gradient approximation and balanced tropical moisture waves. *J. Atmos. Sci.*, **58**, 3650–3665, doi:10.1175/1520-0469(2001)058<3650:TWTGAA>2.0.CO;2.
- Song, X., and G. J. Zhang, 2014: Role of climate feedback in El Niño-like SST response to global warming. *J. Climate*, **27**, 7301–7318, doi:10.1175/JCLI-D-14-00072.1.
- Tang, B. H., and J. D. Neelin, 2004: ENSO Influence on Atlantic hurricanes via tropospheric warming. *Geophys. Res. Lett.*, **31**, L24204, doi:10.1029/2004GL021072.
- Teng, H., L. E. Buja, and G. A. Meehl, 2006: Twenty-first-century climate change commitment from a multi-model ensemble. *Geophys. Res. Lett.*, **33**, L07706, doi:10.1029/2005GL024766.
- Trenberth, K. E., 1997: The definition of El Niño. *Bull. Amer. Meteor. Soc.*, **78**, 2771–2777, doi:10.1175/1520-0477(1997)078<2771:TDOENO>2.0.CO;2.
- Tsintikidis, D., and G. J. Zhang, 1998: A numerical study on the coupling between sea surface temperature and surface evaporation. *J. Geophys. Res.*, **103**, 31 763–31 774, doi:10.1029/1998JD200027.
- Ward, M. N., 1998: Diagnosis and short-lead time prediction of summer rainfall in tropical North Africa at interannual and multidecadal timescales. *J. Climate*, **11**, 3167–3191, doi:10.1175/1520-0442(1998)011<3167:DASLTP>2.0.CO;2.
- Weller, E., and W. Cai, 2013: Asymmetry in the IOD and ENSO teleconnection in a CMIP5 model ensemble and its relevance to regional rainfall. *J. Climate*, **26**, 5139–5149, doi:10.1175/JCLI-D-12-00789.1.
- Xavier, P. K., C. Marzin, and B. N. Goswami, 2007: An objective definition of the Indian summer monsoon season and a new perspective on the ENSO–monsoon relationship. *Quart. J. Roy. Meteor. Soc.*, **133**, 749–764, doi:10.1002/qj.45.
- Xie, P., M. Chen, S. Yang, A. Yatagai, T. Hayasaka, Y. Fukushima, and C. Liu, 2007: A gauge-based analysis of daily precipitation over East Asia. *J. Hydrometeorol.*, **8**, 607–626, doi:10.1175/JHM583.1.
- Yeh, S.-W., Y.-G. Ham, and J.-Y. Lee, 2012: Changes in the tropical Pacific SST trend from CMIP3 to CMIP5 and its implication of ENSO. *J. Climate*, **25**, 7764–7771, doi:10.1175/JCLI-D-12-00304.1.
- Zeng, N., J. D. Neelin, K. M. Lau, and C. J. Tucker, 1999: Enhancement of interdecadal climate variability in the Sahel by vegetation interaction. *Science*, **286**, 1537–1540, doi:10.1126/science.286.5444.1537.